Lattice determination of the spectral function for $D_s \to l\nu_l\gamma^*$ decays

Giuseppe Gagliardi, INFN Sezione di Roma Tre

R. Frezzotti, V. Lubicz, G. Martinelli, F. Mazzetti, C.T. Sachrajda,
F. Sanfilippo, S. Simula, N. Tantalo

NeΨ 23, 16 February 2023, Pisa.

Outline of the talk

Introduction

- Sketch of the problem of the analytic continuation for hadronic amplitudes above kinematical thresholds.
- Spectral density methods as a way-out to the problem.

The HLT method to reconstruct smeared hadronic amplitudes

- Brief description of the method.
- The reconstruction at work in a simple toy model.

Smeared amplitudes for $D_s^{\pm} \to l'^{+} l'^{-} l^{\pm} \nu_l$ decays

- Proof-of-principle calculation at $a \sim 0.08$ fm.

Off-topic(?): The real photon case, i.e. $D_s \to l \nu_l \gamma$.

- Full calculation of the axial and vector form factors F_A and F_V.

Introduction

General statement of the problem (I)

An hadronic amplitude $H(E)$ can be safely extracted on the lattice only for energy E smaller than the energies of all the intermediate states contributing to $H(E)$.

E.g. consider an hadronic amplitude of the form

$$H(E) = \int_0^\infty dt\, e^{iEt}\, C(t), \quad C(t) \equiv \langle 0 | T\{J_A(t) J_B(0)\} | P \rangle \overset{t \geq 0}{=} \sum_{n=0}^{\infty} C_n\, e^{-iE_n t}$$

with J_A, J_B arbitrary currents and $|P\rangle$ an hadronic state.

If $E < E_n$ safe analytic continuation from Minkowskian to Euclidean space

$$H(E) = \int_0^\infty dt\, e^{iEt}\, C(t) \overset{\tau = it}{=}$$

$$= -i \int_0^\infty d\tau\, e^{E\tau}\, C(-i\tau)$$

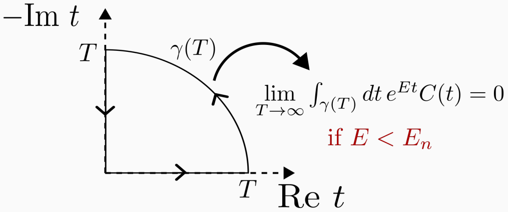

General statement of the problem (II)

On a finite lattice, where non-analiticities are absent, we can access $C_E(t) \equiv C(-it)$ for $0 \le t \le T$.

$$H^T(E) = -i \int_0^T dt\, e^{Et}\, C_E(t) = -i \sum_{n=0}^{\infty} C_n \, \frac{1 - e^{-(E_n - E)T}}{E_n - E}$$

if $E < E_n$:

$$H^T(E) \underset{T\to\infty}{\rightarrow} -i \sum_{n=0}^{\infty} \frac{C_n}{E_n - E}$$

✓

if $E_0 < E$:

$$H^T(E) \underset{T\to\infty}{\rightarrow} -i \sum_{n=0}^{\infty} \frac{C_n}{E_n - E} + \sum_{n}^{E_n < E} iC_n \frac{e^{(E-E_n)T}}{E - E_n}$$

✗

- For $E_0 < E$ dominant $T-$divergent part of $H^T(E)$ must be subtracted $\implies$ difficult in presence of statistical errors, problem worsens when many states E_n below energy E.
- Above threshold hadronic amplitudes become complex (for $E = E_n$). How do we get imaginary parts?

Hadronic amplitudes via the spectral representation (I)

The spectral density $\rho(E')$ of the correlator $C(t > 0)$ is defined as

$$\rho(E') = \langle 0 \big| J_A(0)\, \delta(\mathcal{H} - E')\, J_B(0) \big| P \rangle$$

- $\mathcal{H}$ is the QCD Hamiltonian. One has

$$C(t) \overset{t \geq 0}{=} \int_0^\infty dE'\, \rho(E')\, e^{-iE't}, \qquad C_E(t) \overset{t \geq 0}{=} \int_0^\infty dE'\, \rho(E')\, e^{-E't}$$

- The hadronic amplitude $H(E)$ can be computed as

$$H(E) = \lim_{\epsilon \to 0} -i \int_0^\infty dE'\, \rho(E') \int_0^\infty dt\, e^{-i(E'-E)t} f(\epsilon, t)$$

- $f(\epsilon, t)$ is any regulator for the time integral, with $f(0, t) = 1$.

- E.g. $f(\epsilon, t) = \exp(-\epsilon t)$, $\exp(-\epsilon^2 t^2/2)$. Using standard $\epsilon-$prescription:

$$iH(E) = \lim_{\epsilon \to 0} \int_0^\infty dE'\, \frac{\rho(E')}{E' - E - i\epsilon}$$

Hadronic amplitudes via the spectral representation (II)

From the knowledge of $\rho(E')$, the real and imaginary part of $iH(E)$ can be computed:

$$\mathrm{Re}\,[iH(E)] = \lim_{\epsilon\to 0}\int_0^\infty dE'\,\rho(E')\,\frac{E'-E}{(E-E')^2+\epsilon^2} = \mathrm{P.V.}\int_0^\infty dE'\,\frac{\rho(E')}{E'-E}$$

$$\mathrm{Im}\,[iH(E)] = \lim_{\epsilon\to 0}\int_0^\infty dE'\,\rho(E')\,\frac{\epsilon}{(E-E')^2+\epsilon^2} = \pi\rho(E)$$

For $E < E_0$, since $\rho(E) = 0$, $\mathrm{Im}\,[iH(E)] = 0$ and the $\mathrm{P.V.}$ can be dropped:

$$\mathrm{Re}\,[iH(E)] = \int_{E_0}^\infty dE'\rho(E')\underbrace{\int_0^\infty dt\,e^{-(E'-E)t}}_{=(E'-E)^{-1}\ \text{if}\ E'<E} = \int_0^\infty dt\,e^{Et}\,C_E(t)$$ ✓

For $E > E_0$, $\lim \epsilon \to 0$ can be taken only after evaluating the energy integral.

We propose to employ the previous representation to evaluate the smeared amplitudes $\mathrm{Re}\,[iH(E,\epsilon)]$,$\mathrm{Im}\,[iH(E,\epsilon)]$ at finite ϵ, and then take $\lim \epsilon \to 0$.

The HLT method to reconstruct smeared hadronic amplitudes

The problem of numerically-inverting the Laplace transform

The spectral density $\rho(E')$ is related to our lattice input $C_E(t)$ through an inverse Laplace transform:

$$C_E(t) \overset{t\geq 0}{=} \int_0^\infty dE'\, e^{-E't}\, \rho(E') \implies \rho(E') = \mathcal{L}^{-1}\{C_E\}(E')$$

- Evaluating $\mathcal{L}^{-1}$ is an ill-posed problem if $C_E(t)$ known only on a finite set of points and with a finite accuracy [typical situation in a lattice calculation].
- Evaluating the convolution of $\rho(E')$ with the $\epsilon-$kernels [what QFT dictates]:

$$K_{\rm Re}(x,\epsilon) = \frac{x}{x^2+\epsilon^2}\,, \qquad K_{\rm Im}(x,\epsilon) = \frac{\epsilon}{x^2+\epsilon^2}$$

  is instead a well-posed problem at non-zero ϵ [G. Backus & F. Gilbert 1968].

- The HLT method: find for fixed E and ϵ the best approximation to $K_{\rm Re/Im}(E'-E,\epsilon)$ in terms of $b_t(E') \equiv \exp(-E't)^*$:

$$K_{\rm Re}(E'-E,\epsilon) \simeq \sum_{t=t_{\rm min}}^{t_{\rm max}} g_{\rm Re}(t,E,\epsilon)\cdot b_t(E')\,, \quad K_{\rm Im}(E'-E,\epsilon) \simeq \sum_{t=t_{\rm min}}^{t_{\rm max}} g_{\rm Im}(t,E,\epsilon)\cdot b_t(E')$$

in such a way to optimize the balance between systematic and statistical errors [M. Hansen, A. Lupo, N. Tantalo 2019]. ($^*E', E, \epsilon$ and $t \in \mathbb{N}$ intended now in lattice units!)

The HLT method

$$\text{Re}\,[iH(E,\epsilon)] \simeq \sum_{t=t_{\min}}^{t_{\max}} C_E(t)\, g_{\text{Re}}(t,E,\epsilon), \quad \text{Im}\,[iH(E,\epsilon)] \simeq \sum_{t=t_{\min}}^{t_{\max}} C_E(t)\, g_{\text{Im}}(t,E,\epsilon)$$

In the HLT, best coefficients $g_r(t,E,\epsilon)$, $r = \{\text{Re},\text{Im}\}$, obtained minimizing

$$W_r[\boldsymbol{g}] = (1-\lambda)\frac{A_r[\boldsymbol{g}]}{A_r[\boldsymbol{0}]} + \frac{\lambda}{C_E^2(0)} B[\boldsymbol{g}]\,, \quad \lambda \in [0,1]$$

$$\underbrace{A_r[\boldsymbol{g}] = \int_{E_{th}}^{\infty} dE' \left| K_r(E'-E,\epsilon) - \sum_{t=t_{\min}}^{t_{\max}} g(t)\, b_t(E') \right|^2}_{\text{syst. error on kernel reconstruction}}, \quad \underbrace{B[\boldsymbol{g}] = \sum_{t,t'=t_{\min}}^{t_{\max}} g(t) \overbrace{\text{Cov}_{C_E}(t,t')}^{\text{covariance matrix of } C_E} g(t')}_{\text{stat. error on Re}[iH(E,\epsilon)],\ \text{Im}[iH(E,\epsilon)]}$$

- λ is the trade-off parameter, when $\lambda \simeq 1$ very poor kernel reconstruction.
- For $\lambda \simeq 0$ accurate kernel reconstruction, $g(t)$ typically large in magnitude and oscillating $\implies$ large stat. errors induced on $iH(E,\epsilon)$.
- $\implies$ find the optimal value λ^* where stat. and syst. are balanced and results stable under variations of $\lambda \sim \lambda^*$.

The reconstruction at work in a toy-model without errors

Two-resonances model:

$$\rho(E) = \frac{1}{\pi} \sum_{n=1,2} \frac{\Gamma_n}{(E-E_n)^2 + \Gamma_n^2}\,, \qquad \begin{aligned} E_1 &= 0.10,\ \Gamma_1 = 5\cdot 10^{-3} \\ E_2 &= 0.15,\ \Gamma_2 = 10^{-2} \end{aligned}$$

- We computed $C_E(t)$ with extended machine precision for $t = 1, \ldots, 200$.
- $H(E,\epsilon)$ reconstructed from $C_E(t)$ using the HLT method with $B[\boldsymbol{g}] = 0$.

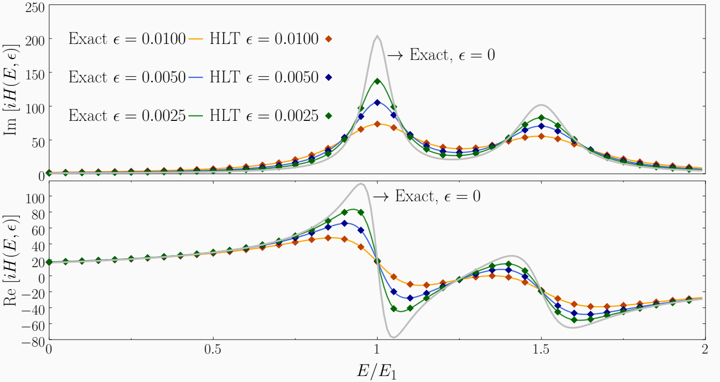

The reconstruction at work in a toy-model without errors

Two-resonances model:

$$\rho(E) = \frac{1}{\pi} \sum_{n=1,2} \frac{\Gamma_n}{(E-E_n)^2 + \Gamma_n^2}\,, \qquad \begin{aligned} E_1 &= 0.10,\ \Gamma_1 = 5\cdot 10^{-3} \\ E_2 &= 0.15,\ \Gamma_2 = 10^{-2} \end{aligned}$$

- We computed $C_E(t)$ with extended machine precision for $t = 1, \ldots, 200$.
- $H(E,\epsilon)$ reconstructed from $C_E(t)$ using the HLT method with $B[\boldsymbol{g}] = 0$.

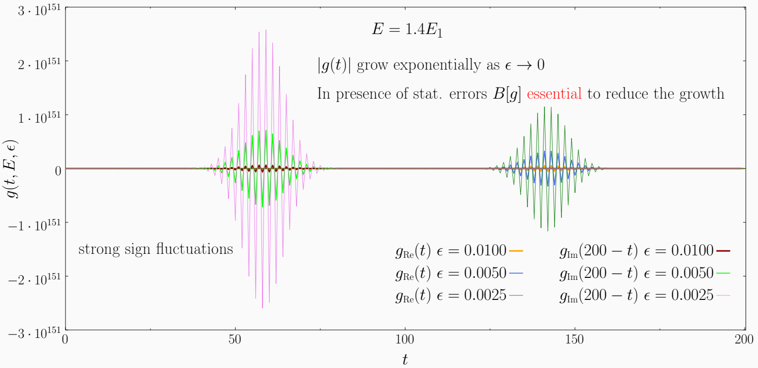

Smeared amplitudes for $D_s^{\pm} \to l'^{+} l'^{-} l^{\pm} \nu_l$ decays

Relevant Feynman diagrams for the process

The $P^+ \equiv \bar{D}\gamma^5 U \to l'^+ l'^- l^+ \nu_l$ decays

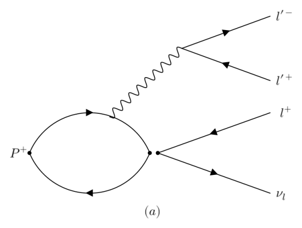

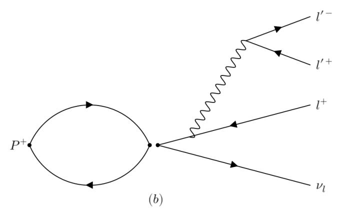

- Diagram (b) is perturbative, only QCD input is decay constant f_P.
- Diagram (a) is non-perturbative. Virtual photon γ^* emitted from either a $U-$type or a $D-$type quark line. For $P^+ = D_s^+$: $U = c$, $D = s$.

Non-perturbative QCD contribution encoded in the hadronic tensor

$$H_W^{\mu\nu}(k, \boldsymbol{p}) = \int d^4x\, e^{ik\cdot x} \left\langle 0 \middle| T[J^\mu_{\rm em}(x) J^\nu_W(0)] \middle| P(\boldsymbol{p}) \right\rangle, \quad W = V, A$$

- $k = (E_\gamma, \boldsymbol{k})$ is photon 4-momentum, $\boldsymbol{p}$ is P-meson 3-momentum.
- We neglect $\mathrm{SU}(3)$-vanishing quark-line disconnected diagrams.

Threshold problem at large virtualities k^2

$$H_W^{\mu\nu}(k,0) = \int_{-\infty}^{\infty} dt\, e^{iE_\gamma t} \left\langle 0 \middle| T[J_{\rm em}^\mu(t,\boldsymbol{k}) J_W^\nu(0)] \middle| P(\boldsymbol{0}) \right\rangle =$$

$$= \underbrace{\int_{-\infty}^{0} dt\, e^{iE_\gamma t} \left\langle 0 \middle| J_W^\nu(0) J_{\rm em}^\mu(t,\boldsymbol{k}) \middle| P(\boldsymbol{0}) \right\rangle}_{H_{W,1}^{\mu\nu}(k)} + \underbrace{\int_{0}^{\infty} dt\, e^{iE_\gamma t} \left\langle 0 \middle| J_{\rm em}^\mu(t,\boldsymbol{k}) J_W^\nu(0) \middle| P(\boldsymbol{0}) \right\rangle}_{H_{W,2}^{\mu\nu}(k)}$$

Inserting a complete set of states between the two currents:

$$H_{W,1}^{\mu\nu}(k) = -i \sum_r \frac{\langle 0|J_W^\nu(0)|r\rangle\langle r|J_{\rm em}^\mu(\boldsymbol{k})|P(\boldsymbol{0})\rangle}{E_r + E_\gamma - M_P - i\epsilon}, \quad \boldsymbol{p}_r = -\boldsymbol{k}, \quad |r\rangle = \bar{D}\gamma^\nu U,\ \bar{D}\gamma^\nu\gamma^5 U$$

$$H_{W,2}^{\mu\nu}(k) = -i \sum_n \frac{\langle 0|J_{\rm em}^\mu(\boldsymbol{k})|n\rangle\langle n|J_W^\nu(0)|P(\boldsymbol{0})\rangle}{E_n - E_\gamma - i\epsilon}, \quad \boldsymbol{p}_n = +\boldsymbol{k}, \quad |n\rangle = \bar{D}\gamma^\mu D,\ \bar{U}\gamma^\mu U$$

- 1st TO: $E_r \geq \sqrt{M_P^2 + |\boldsymbol{k}|^2} \implies E_r + E_\gamma - M_P \geq 0$ ✓.
- 2nd TO: $E_n - E_\gamma < 0$ if $\sqrt{k^2} > M_n$ [mass of the vector state $|n\rangle$] ✗.

Threshold at: $\sqrt{k_{th}^2} = \min(M_{V_U}, M_{V_D}) \implies E_{\gamma,th} = \sqrt{k_{th}^2 + |\boldsymbol{k}|^2}$.

M_{V_f} is the mass of the lightest $\bar{f}\gamma^\mu f$ state. For $P^+ = D_s^+$, $M_{V_s} = M_\phi$, $M_{V_c} = M_{J/\Psi}$.

The hadronic tensor from Euclidean lattice correlators

$H_W^{\mu\nu}$ can be extracted from the following Euclidean three-point function evaluated on a $L^3 \times T$ lattice:

$$M_W^{\mu\nu}(t, t_W, \boldsymbol{k}) \equiv T \langle J_{\text{em}}^{\mu}(t + t_W, \boldsymbol{k}) \; J_W^{\nu}(t_W) \; \hat{P}(0) \rangle_{LT}$$

- $\hat{P}$ is an interpolator for the $P^+(\mathbf{0})$ meson, inserted at Euclidean time 0.
- Weak current placed at a fixed Euclidean time t_W.
- To ensure ground-state dominance, t_W must be chosen sufficiently large.
- We employ local weak current J_W and local/conserved e.m. current J_{em}.

Up to a normalization factor $\mathcal{N}(t_W)$ and finite-t_W corrections:

$$C_{W,1}^{\mu\nu}(t, \boldsymbol{k}) \equiv \langle 0 \big| J_W^{\nu}(0) \; J_{\text{em}}^{\mu}(t, \boldsymbol{k}) \big| P(\mathbf{0}) \rangle \overset{t \leq 0}{=} \frac{1}{\mathcal{N}(t_W)} M_W^{\mu\nu}(\boldsymbol{k}, t, t_W)$$

$$C_{W,2}^{\mu\nu}(t, \boldsymbol{k}) \equiv \langle 0 \big| J_{\text{em}}^{\mu}(t, \boldsymbol{k}) \; J_W^{\nu}(0) \big| P(\mathbf{0}) \rangle \overset{t \geq 0}{=} \frac{1}{\mathcal{N}(t_W)} M_W^{\mu\nu}(\boldsymbol{k}, t, t_W)$$

Proof-of-principle calculation for $P = D_s$

We evaluated $M_W^{\mu\nu}(t, t_W, \boldsymbol{k})$ on a single $N_f = 2+1+1$ Wilson-clover twisted-mass ETMC gauge ensemble at the physical point

Ensemble	a [fm]	L/a	T/a	t_W/a	N_{confs}	N_{sources}
cB211.072.64	0.079	64	128	22 [25*]	302	4

*Analyzed with limited statistics, only used to check ground-state isolation (Backup).

- $\boldsymbol{k}$ along $z-$axis, simulated $x_\gamma \equiv 2|\boldsymbol{k}|/M_{D_s} : 0.2, 0.5, 0.7$.
- Implemented $\boldsymbol{k}$, $-\boldsymbol{k}$ average $\Longrightarrow$ effective noise reduction at small x_γ.
- Analyzed separately the s- and c-quark contrib. to $C_{W,1}^{\mu\nu}$ and $C_{W,2}^{\mu\nu}$.
- Threshold problems only in s-quark contrib. $C_{W,2}^{\mu\nu;s}$ for $\sqrt{k^2} > M_\phi$.

From $C_{W;2}^{\mu\nu;s}$, we evaluate the smeared amplitudes employing the HLT method

$$\text{Re/Im}\,[iH_{W,2}^{\mu\nu;s}(E_\gamma, \boldsymbol{k}, \epsilon)] = \int_0^\infty dE'\,\rho_{W,2}^{\mu\nu;s}(E', \boldsymbol{k})\,K_{\text{Re/Im}}(E' - E_\gamma, \epsilon)$$

$$C_{W,2}^{\mu\nu;s}(t, \boldsymbol{k}) = \int_0^\infty dE'\,\rho_{W,2}^{\mu\nu;s}(E', \boldsymbol{k})\,e^{-E't}$$

Vector part of the hadronic tensor [H_V given in lattice units]

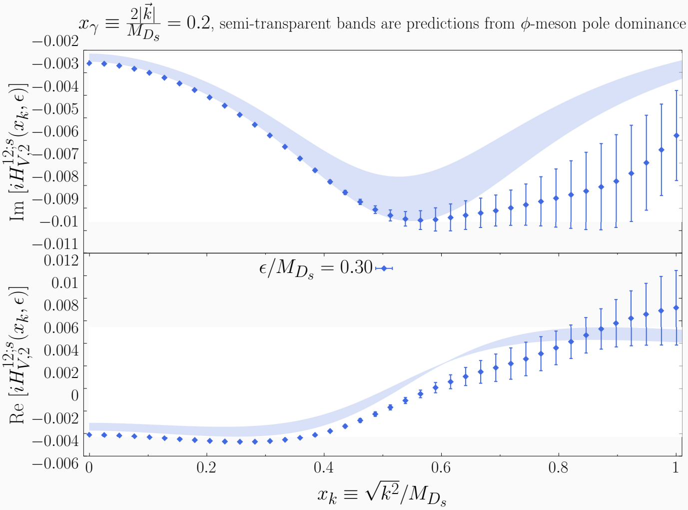

Kernels adopted $x \equiv a(E - E_\gamma)$ [tend to previous kernels in the limit $a \to 0$]:

$$K_{\mathrm{Re}}(x, a\epsilon) = \frac{2e^{-x}\sinh(x/2)}{4\sinh^2(x/2) + (a\epsilon)^2}, \qquad K_{\mathrm{Im}}(x, a\epsilon) = \frac{(a\epsilon)e^{-x}}{4\sinh^2(x/2) + (a\epsilon)^2}$$

Vector part of the hadronic tensor [H_V given in lattice units]

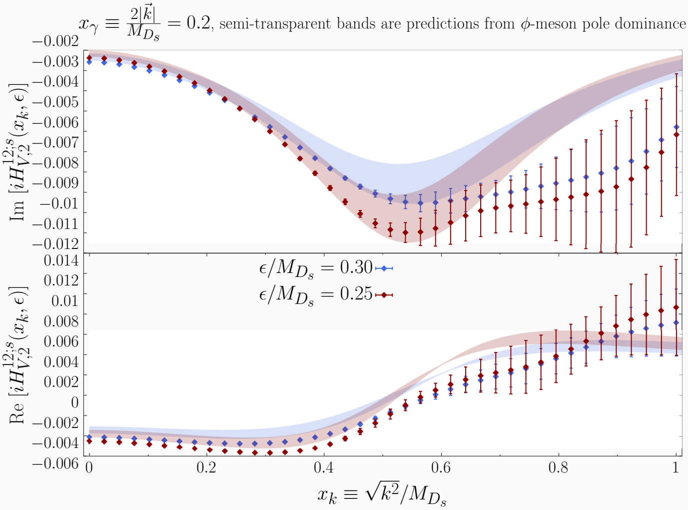

Kernels adopted $x \equiv a(E - E_\gamma)$ [tend to previous kernels in the limit $a \to 0$]:

$$K_{\mathrm{Re}}(x, a\epsilon) = \frac{2e^{-x}\sinh(x/2)}{4\sinh^2(x/2) + (a\epsilon)^2}, \qquad K_{\mathrm{Im}}(x, a\epsilon) = \frac{(a\epsilon)e^{-x}}{4\sinh^2(x/2) + (a\epsilon)^2}$$

Vector part of the hadronic tensor [H_V given in lattice units]

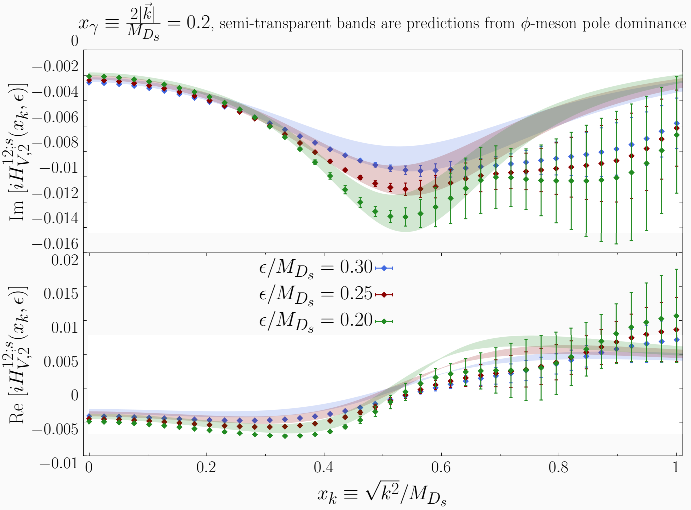

Kernels adopted $x \equiv a(E - E_\gamma)$ [tend to previous kernels in the limit $a \to 0$]:

$$K_{\mathrm{Re}}(x, a\epsilon) = \frac{2e^{-x}\sinh(x/2)}{4\sinh^2(x/2) + (a\epsilon)^2}, \qquad K_{\mathrm{Im}}(x, a\epsilon) = \frac{(a\epsilon)e^{-x}}{4\sinh^2(x/2) + (a\epsilon)^2}$$

Vector part of the hadronic tensor [H_V given in lattice units]

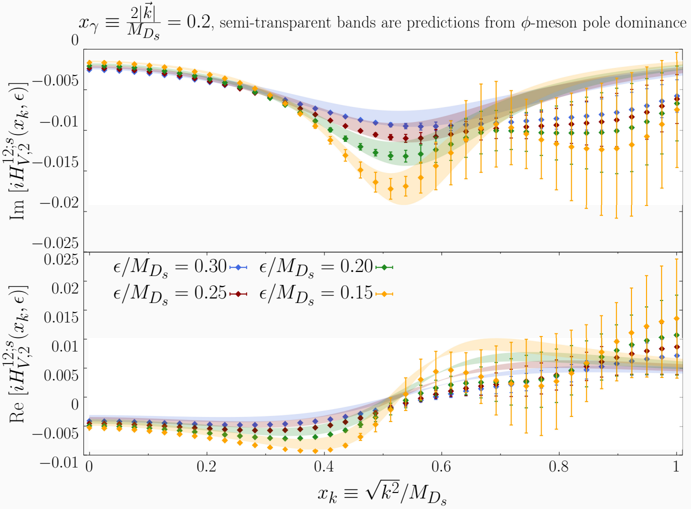

Kernels adopted $x \equiv a(E - E_\gamma)$ [tend to previous kernels in the limit $a \to 0$]:

$$K_{\mathrm{Re}}(x, a\epsilon) = \frac{2e^{-x}\sinh(x/2)}{4\sinh^2(x/2) + (a\epsilon)^2}, \qquad K_{\mathrm{Im}}(x, a\epsilon) = \frac{(a\epsilon)e^{-x}}{4\sinh^2(x/2) + (a\epsilon)^2}$$

Vector part of the hadronic tensor [H_V given in lattice units]

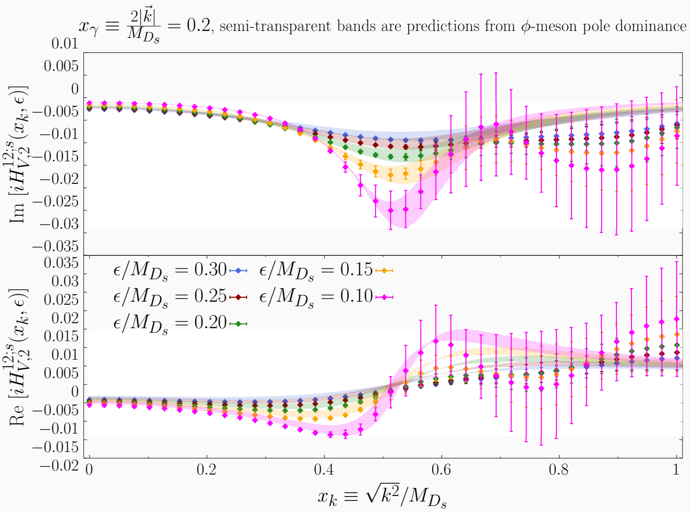

Kernels adopted $x \equiv a(E - E_\gamma)$ [tend to previous kernels in the limit $a \to 0$]:

$$K_{\mathrm{Re}}(x, a\epsilon) = \frac{2e^{-x}\sinh(x/2)}{4\sinh^2(x/2) + (a\epsilon)^2}, \qquad K_{\mathrm{Im}}(x, a\epsilon) = \frac{(a\epsilon)e^{-x}}{4\sinh^2(x/2) + (a\epsilon)^2}$$

Vector part of the hadronic tensor [H_V given in lattice units]

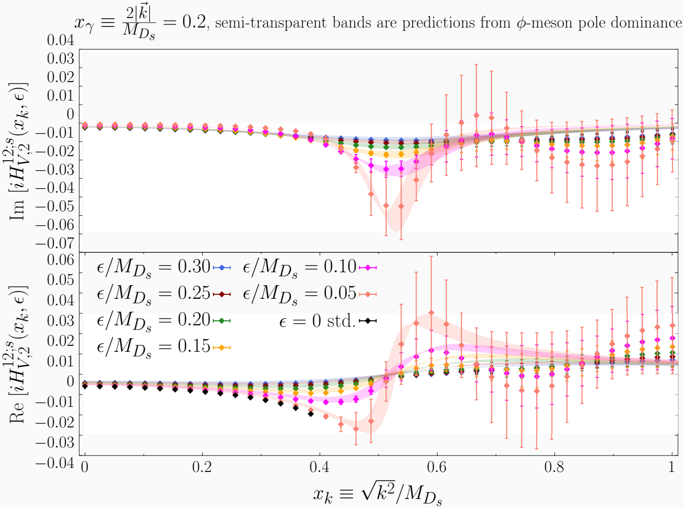

Kernels adopted $x \equiv a(E - E_\gamma)$ [tend to previous kernels in the limit $a \to 0$]:

$$K_{\mathrm{Re}}(x, a\epsilon) = \frac{2e^{-x}\sinh(x/2)}{4\sinh^2(x/2) + (a\epsilon)^2}, \qquad K_{\mathrm{Im}}(x, a\epsilon) = \frac{(a\epsilon)e^{-x}}{4\sinh^2(x/2) + (a\epsilon)^2}$$

Axial part of the hadronic tensor [H_A given in lattice units]

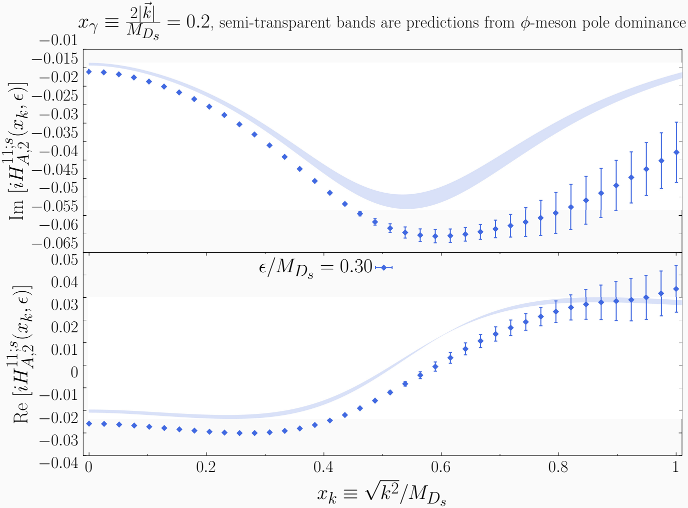

Kernels adopted $x \equiv a(E - E_\gamma)$ [tend to previous kernels in the limit $a \to 0$]:

$$K_{\mathrm{Re}}(x, a\epsilon) = \frac{2e^{-x}\sinh(x/2)}{4\sinh^2(x/2) + (a\epsilon)^2}, \qquad K_{\mathrm{Im}}(x, a\epsilon) = \frac{(a\epsilon)e^{-x}}{4\sinh^2(x/2) + (a\epsilon)^2}$$

Axial part of the hadronic tensor [H_A given in lattice units]

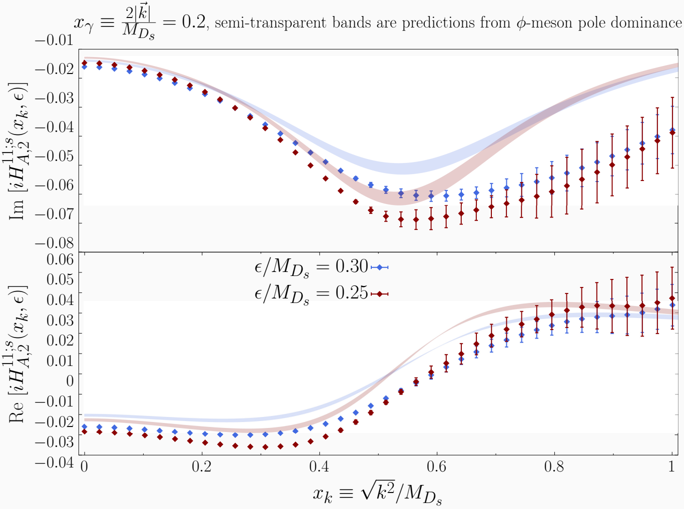

Kernels adopted $x \equiv a(E - E_\gamma)$ [tend to previous kernels in the limit $a \to 0$]:

$$K_{\mathrm{Re}}(x, a\epsilon) = \frac{2e^{-x}\sinh(x/2)}{4\sinh^2(x/2) + (a\epsilon)^2}, \qquad K_{\mathrm{Im}}(x, a\epsilon) = \frac{(a\epsilon)e^{-x}}{4\sinh^2(x/2) + (a\epsilon)^2}$$

Axial part of the hadronic tensor [H_A given in lattice units]

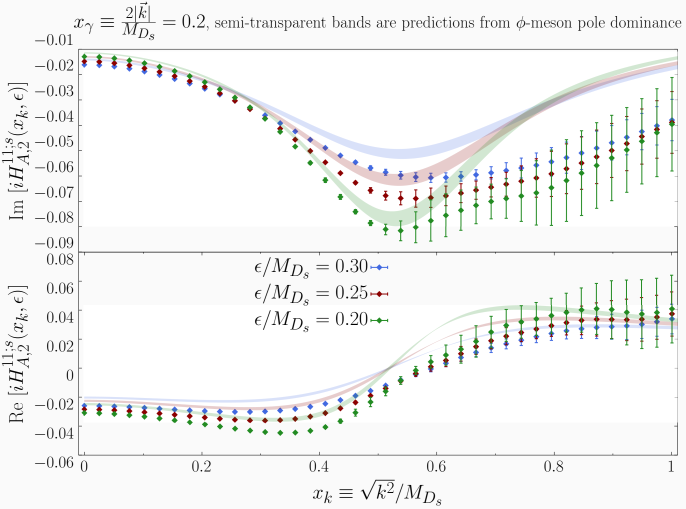

Kernels adopted $x \equiv a(E - E_\gamma)$ [tend to previous kernels in the limit $a \to 0$]:

$$K_{\mathrm{Re}}(x, a\epsilon) = \frac{2e^{-x}\sinh(x/2)}{4\sinh^2(x/2) + (a\epsilon)^2}, \qquad K_{\mathrm{Im}}(x, a\epsilon) = \frac{(a\epsilon)e^{-x}}{4\sinh^2(x/2) + (a\epsilon)^2}$$

Axial part of the hadronic tensor [H_A given in lattice units]

$x_\gamma \equiv \frac{2|\vec{k}|}{M_{D_s}} = 0.2$, semi-transparent bands are predictions from ϕ-meson pole dominance

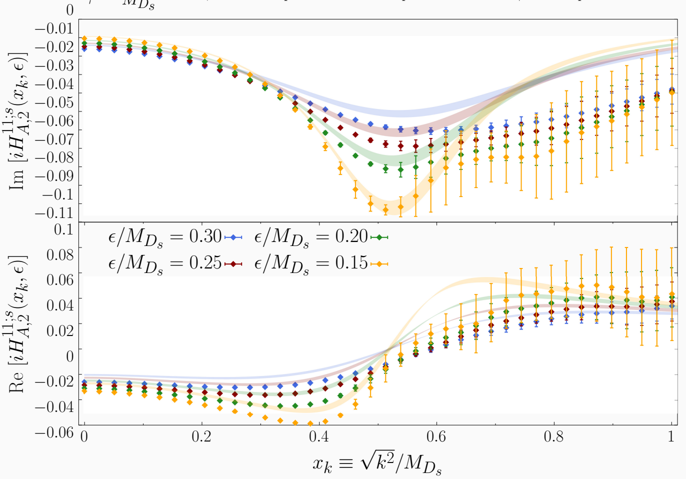

Kernels adopted $x \equiv a(E - E_\gamma)$ [tend to previous kernels in the limit $a \to 0$]:

$$K_{\mathrm{Re}}(x, a\epsilon) = \frac{2e^{-x}\sinh(x/2)}{4\sinh^2(x/2) + (a\epsilon)^2}, \qquad K_{\mathrm{Im}}(x, a\epsilon) = \frac{(a\epsilon)e^{-x}}{4\sinh^2(x/2) + (a\epsilon)^2}$$

Axial part of the hadronic tensor [H_A given in lattice units]

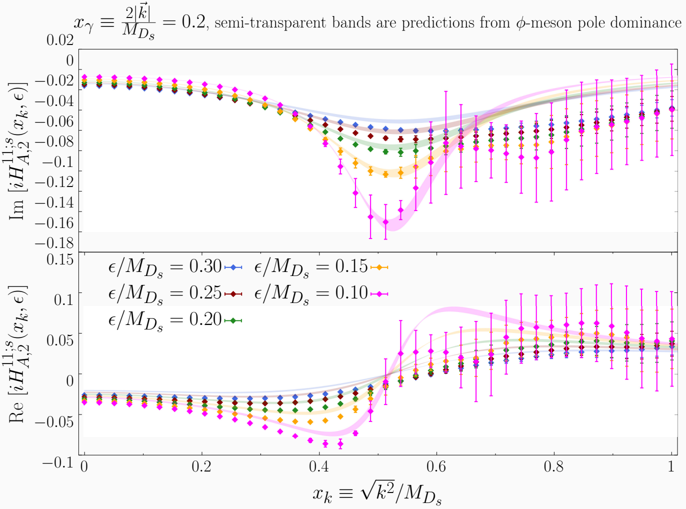

Kernels adopted $x \equiv a(E - E_\gamma)$ [tend to previous kernels in the limit $a \to 0$]:

$$K_{\mathrm{Re}}(x, a\epsilon) = \frac{2e^{-x}\sinh(x/2)}{4\sinh^2(x/2) + (a\epsilon)^2}, \qquad K_{\mathrm{Im}}(x, a\epsilon) = \frac{(a\epsilon)e^{-x}}{4\sinh^2(x/2) + (a\epsilon)^2}$$

Axial part of the hadronic tensor [H_A given in lattice units]

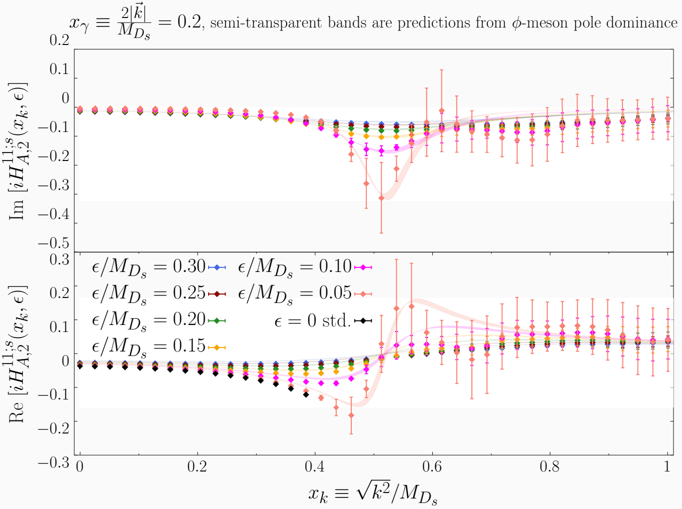

Kernels adopted $x \equiv a(E - E_\gamma)$ [tend to previous kernels in the limit $a \to 0$]:

$$K_{\mathrm{Re}}(x, a\epsilon) = \frac{2e^{-x}\sinh(x/2)}{4\sinh^2(x/2) + (a\epsilon)^2}, \qquad K_{\mathrm{Im}}(x, a\epsilon) = \frac{(a\epsilon)e^{-x}}{4\sinh^2(x/2) + (a\epsilon)^2}$$

Dependence on $x_\gamma \equiv 2|\boldsymbol{k}|/M_{D_s}$

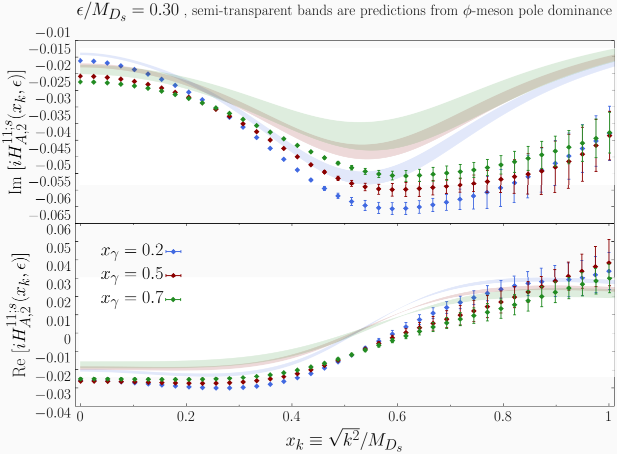

- From $H_W^{\mu\nu}(x_k, \boldsymbol{k})$ at different $\boldsymbol{k}$ (covering the physical interval $x_\gamma \in [0,1]$) one can obtain the total decay rate $\Gamma[D_s \to \bar{l}' l' l \nu_l]$ [G.G. et al, arXiv:2202.03833].
- We plan to evaluate the decay rates $\Gamma(\epsilon)$ using the smeared $H_W^{\mu\nu}(x_k, \boldsymbol{k}, \epsilon)$, and then extrapolate to vanishing ϵ.

Dependence on $x_\gamma \equiv 2|\boldsymbol{k}|/M_{D_s}$

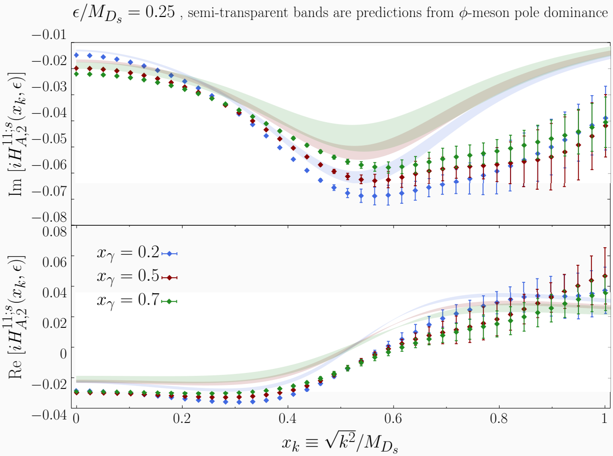

- From $H^{\mu\nu}_W(x_k,\boldsymbol{k})$ at different $\boldsymbol{k}$ (covering the physical interval $x_\gamma \in [0,1]$) one can obtain the total decay rate $\Gamma[D_s \to \bar{l}'l'l\nu_l]$ [G.G. et al, arXiv:2202.03833].
- We plan to evaluate the decay rates $\Gamma(\epsilon)$ using the smeared $H^{\mu\nu}_W(x_k,\boldsymbol{k},\epsilon)$, and then extrapolate to vanishing ϵ.

Dependence on $x_\gamma \equiv 2|\boldsymbol{k}|/M_{D_s}$

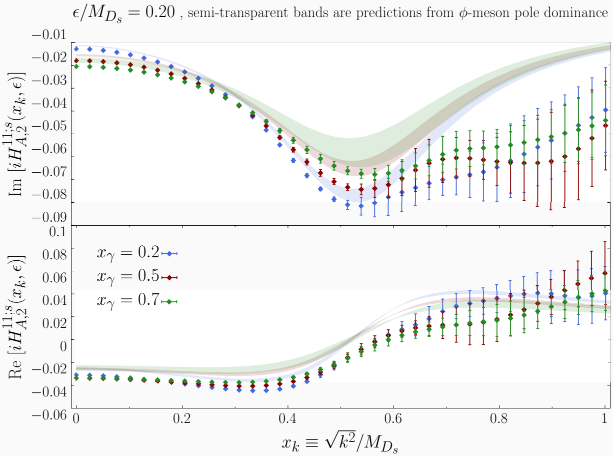

- From $H^{\mu\nu}_W(x_k, \boldsymbol{k})$ at different $\boldsymbol{k}$ (covering the physical interval $x_\gamma \in [0,1]$) one can obtain the total decay rate $\Gamma[D_s \to \bar{l}' l' l \nu_l]$ [G.G. et al, arXiv:2202.03833].
- We plan to evaluate the decay rates $\Gamma(\epsilon)$ using the smeared $H^{\mu\nu}_W(x_k, \boldsymbol{k}, \epsilon)$, and then extrapolate to vanishing ϵ.

Dependence on $x_\gamma \equiv 2|\boldsymbol{k}|/M_{D_s}$

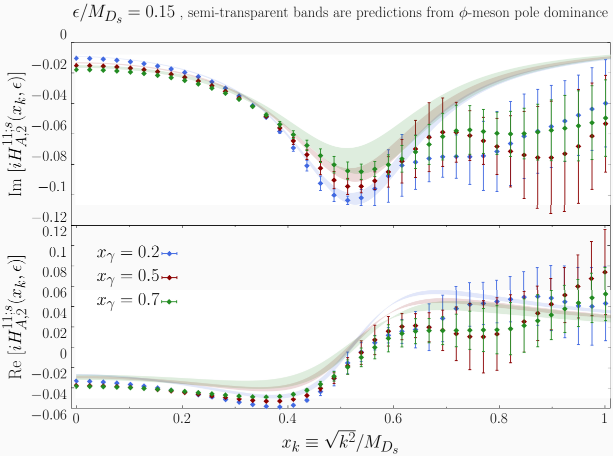

- From $H_W^{\mu\nu}(x_k, \boldsymbol{k})$ at different $\boldsymbol{k}$ (covering the physical interval $x_\gamma \in [0,1]$) one can obtain the total decay rate $\Gamma[D_s \to \bar{l}' l' l \nu_l]$ [G.G. et al, arXiv:2202.03833].
- We plan to evaluate the decay rates $\Gamma(\epsilon)$ using the smeared $H_W^{\mu\nu}(x_k, \boldsymbol{k}, \epsilon)$, and then extrapolate to vanishing ϵ.

Dependence on $x_\gamma \equiv 2|\boldsymbol{k}|/M_{D_s}$

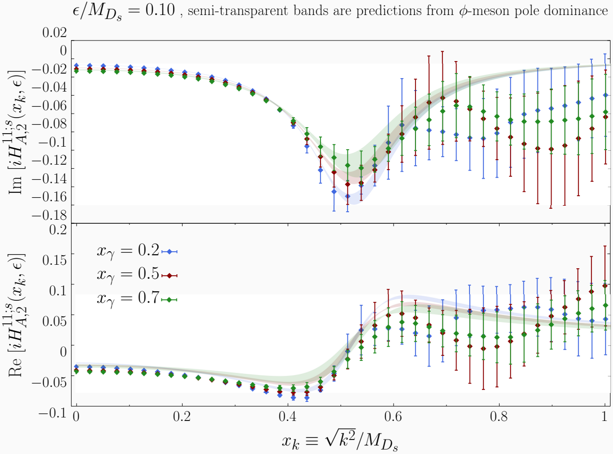

- From $H_W^{\mu\nu}(x_k, \boldsymbol{k})$ at different $\boldsymbol{k}$ (covering the physical interval $x_\gamma \in [0,1]$) one can obtain the total decay rate $\Gamma[D_s \to \bar{l}'l'l\nu_l]$ [G.G. et al, arXiv:2202.03833].
- We plan to evaluate the decay rates $\Gamma(\epsilon)$ using the smeared $H_W^{\mu\nu}(x_k, \boldsymbol{k}, \epsilon)$, and then extrapolate to vanishing ϵ.

Dependence on $x_\gamma \equiv 2|\boldsymbol{k}|/M_{D_s}$

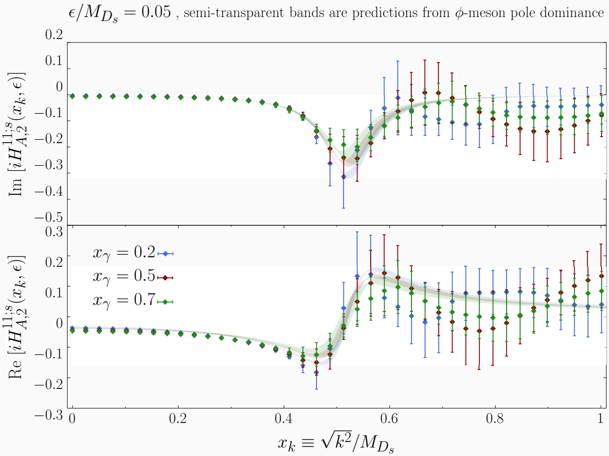

- From $H_W^{\mu\nu}(x_k, \boldsymbol{k})$ at different $\boldsymbol{k}$ (covering the physical interval $x_\gamma \in [0,1]$) one can obtain the total decay rate $\Gamma[D_s \to \bar{l}' l' l \nu_l]$ [G.G. et al, arXiv:2202.03833].
- We plan to evaluate the decay rates $\Gamma(\epsilon)$ using the smeared $H_W^{\mu\nu}(x_k, \boldsymbol{k}, \epsilon)$, and then extrapolate to vanishing ϵ.

A quick update on $D_s \to \ell\nu_\ell\gamma$ [real γ]

Form factors decomposition of $H_W^{\mu\nu}$

The hadronic tensor $H_W^{\mu\nu}$ can be decomposed in term of scalar form factors as

$$
\begin{aligned}
H_W^{\mu\nu}(k,\boldsymbol{p}) &\equiv H_{\rm SD}^{\mu\nu}(k,\boldsymbol{p}) + H_{\rm pt}^{\mu\nu}(k,\boldsymbol{p}) \\
&= \frac{H_1}{M_P}\left[k^2 g^{\mu\nu} - k^\mu k^\nu\right] + \frac{H_2}{M_P}\frac{\left[(p\cdot k - k^2)k^\mu - k^2(p-k)^\mu\right]}{(p-k)^2 - M_P^2}(p-k)^\nu \\
&\quad - i\frac{F_V}{M_P}\varepsilon^{\mu\nu\gamma\beta}k_\gamma p_\beta + \frac{F_A}{M_P}\left[(p\cdot k - k^2)g^{\mu\nu} - (p-k)^\mu k^\nu\right] + H_{\rm pt}^{\mu\nu}(k,\boldsymbol{p})\ . \\
H_{\rm pt}^{\mu\nu}(k,\boldsymbol{p}) &\equiv f_P\left[g^{\mu\nu} + \frac{(2p-k)^\mu(p-k)^\nu}{2p\cdot k - k^2}\right]
\end{aligned}
$$

- M_P, f_P are mass and decay constant of the meson P.
- $H_{SD}^{\mu\nu}$ is the structure-dependent contribution written in terms of three axial form factors H_1, H_2, F_A, and the vector form factor F_V.
- Only F_A and F_V are relevant for $P \to l\nu_l\gamma$. No threshold problems $(k^2 = 0)$.
- In the $P-$meson rest frame and with $\boldsymbol{k}$ along $z-$axis:

$$
F_V(x_\gamma) \propto H_V^{12}(k,0), \qquad F_A(x_\gamma) \propto H_A^{11}(k,0) - \underbrace{H_A^{11}(0,0)}_{\text{point-like subtraction}}
$$

Simulation details

ensemble	β	V/a^4	a (fm)	M_π (MeV)	L (fm)
cA211.12.48	1.726	$48^3 \cdot 96$	0.09075 (54)	174.5 (1.1)	4.36
cB211.072.64	1.778	$64^3 \cdot 128$	0.07957 (13)	140.2 (0.2)	5.09
cC211.060.80	1.836	$80^3 \cdot 160$	0.06821 (13)	136.7 (0.2)	5.46
cD211.054.96	1.900	$96^3 \cdot 192$	0.05692 (12)	140.8 (0.2)	5.46

- Analyzed $\mathcal{O}(100)$ gauge configurations per ensemble (four β considered).
- Spanned the entire kinematical range of $x_\gamma \in [0, 1]$.

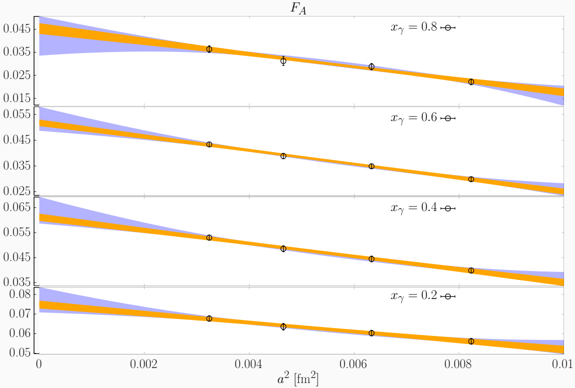

- a^2 (orange) and $a^2 + a^4$ (blue) extrapolation.
- No sign of a^4 cut-off effects.

Continuum extrapolated results [Preliminary]

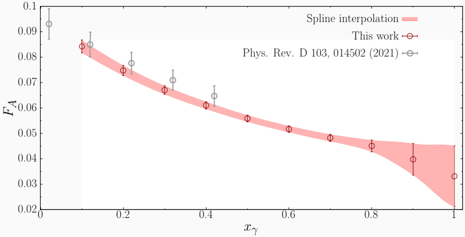

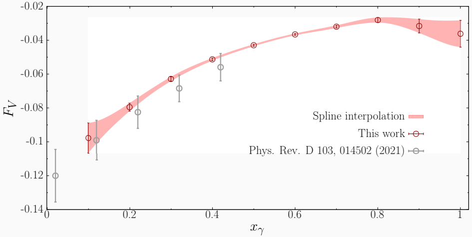

- Sensibly improved the accuracy w.r.t. our previous work.
- Results are still preliminary, very good control on systematics due to continuum extrapolation, but other sources of systematic errors under study.
- Currently we are performing simulations on a $L^3 \times T$ lattice with $L \sim 7$ fm and $T = 2L$, to study both finite$-T$ and finite-volume effects.
- Recently Giusti et al [arXiv:2302.01298] performed a calculation of F_V and F_A on a single RBC/UKQCD ensemble over whole kinematical range. When continuum extrapolated results will be available, interesting comparisons can be made.

Conclusions

- We propose a new method to extract hadronic amplitudes above kinematical thresholds, based on spectral density techniques.
- In our approach, the problem of analytic continuation is bypassed by evaluating, via spectral reconstruction, hadronic amplitudes $H(E,\epsilon)$ smeared over a finite-energy interval ϵ, and then taking $\lim \epsilon \to 0$.
- We performed a pilot-study on a single ETMC ensemble, computing the hadronic tensor $H_W^{\mu\nu}(E,\epsilon)$ relative to $P \to \bar{l}'l'l\nu_l$ decays (below and above threshold(s)) for $\epsilon \in [100 - 600]$ MeV, using the HLT method.

To-do list

- Evaluate differential decay rate $\partial\Gamma[D_s \to \bar{l}'l'l\nu_l]/d|\boldsymbol{k}|$ using smeared hadronic tensor and study ϵ-dependence of $d\Gamma/d|\boldsymbol{k}|$.
- Try to use model calculations as a preconditioner to milden ϵ-dependence: $H(E) = H_{\text{model}}(E,0) + \lim_{\epsilon\to 0}[H(E,\epsilon) - H_{\text{model}}(E,\epsilon)]$.
- Increase number of simulated photon momenta $\boldsymbol{k}$, extend calculation to finer lattice spacings. Try $P = K$, in the future $P = D, B$?

A thank you slide

Thank you for your attention!

Backup

Controlling systematic errors

Stability analysis to find the optimal value of the trade-off parameter $\lambda = \lambda^*$

Below threshold $x_k < x_{k,th} \simeq 0.52$ [No loss of precision at small $A[g]$]

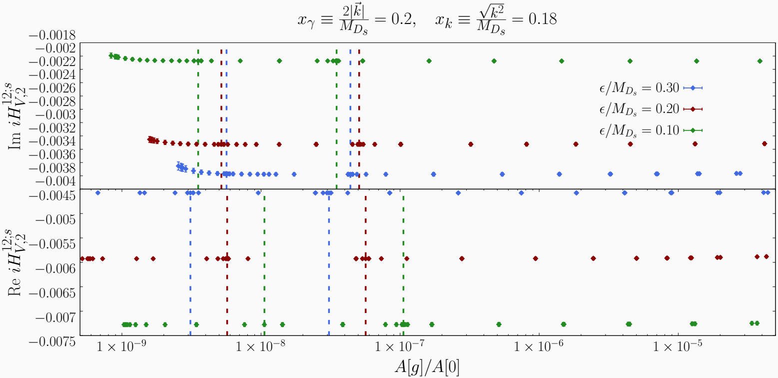

- Rightmost vertical line corresponds to $\lambda = \lambda^*$. Difference w.r.t. value corresponding to leftmost line added as a systematic when significant.
- Reconstruction becomes poorer increasing x_k above threshold and/or decreasing ϵ, as expected.

Controlling systematic errors

Stability analysis to find the optimal value of the trade-off parameter $\lambda = \lambda^*$

Slightly above threshold $x_k \gtrsim x_{k,th} \simeq 0.52$

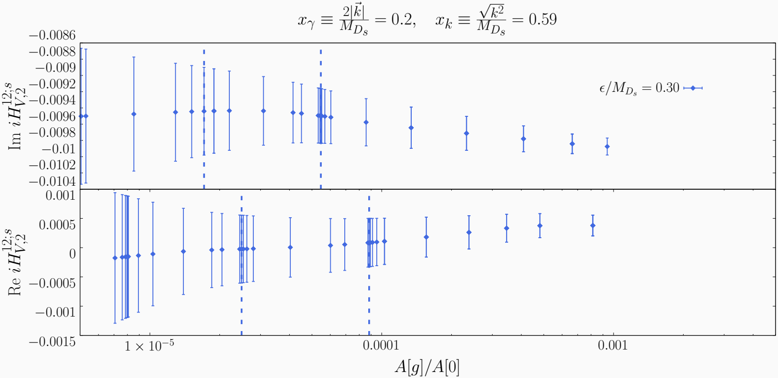

- Rightmost vertical line corresponds to $\lambda = \lambda^*$. Difference w.r.t. value corresponding to leftmost line added as a systematic when significant.
- Reconstruction becomes poorer increasing x_k above threshold and/or decreasing ϵ, as expected.

Controlling systematic errors

Stability analysis to find the optimal value of the trade-off parameter $\lambda = \lambda^*$

Above threshold $x_k > x_{k,th} \simeq 0.52$

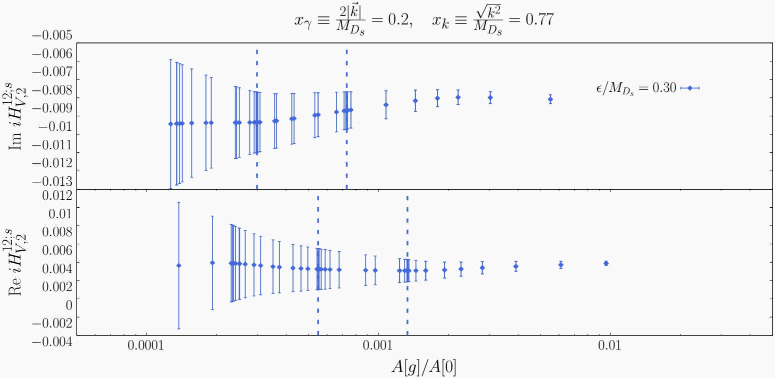

- Rightmost vertical line corresponds to $\lambda = \lambda^*$. Difference w.r.t. value corresponding to leftmost line added as a systematic when significant.
- Reconstruction becomes poorer increasing x_k above threshold and/or decreasing ϵ, as expected.

Local vs conserved electromagnetic current

H_V is given in lattice units

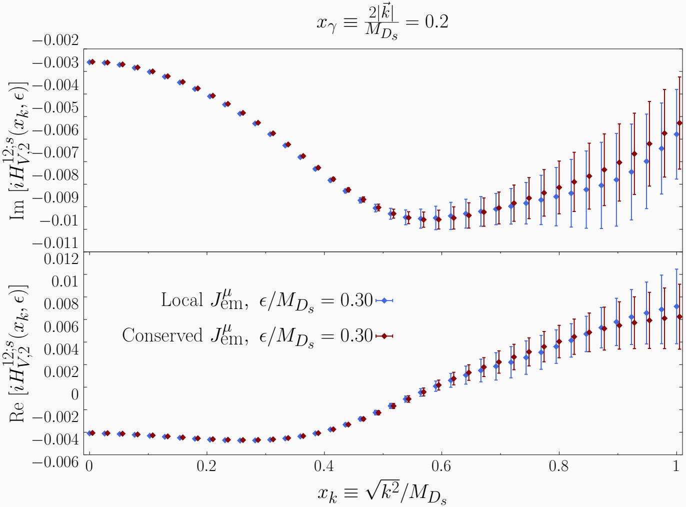

Local vs conserved electromagnetic current

H_V is given in lattice units

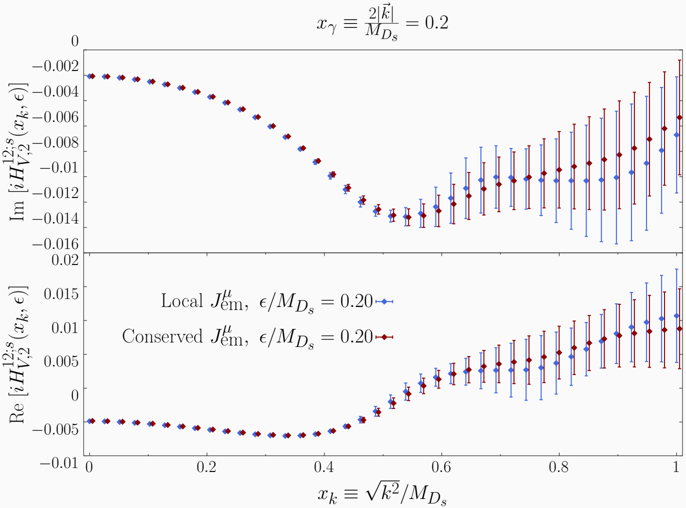

Local vs conserved electromagnetic current

H_V is given in lattice units

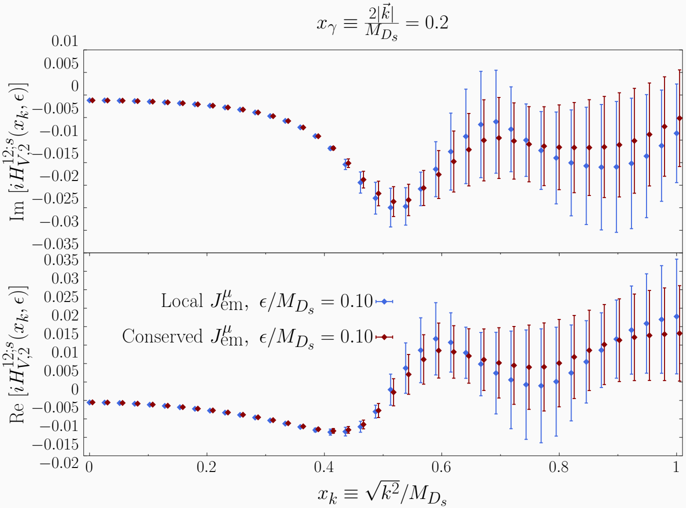

Checking ground-state isolation

H_V is given in lattice units

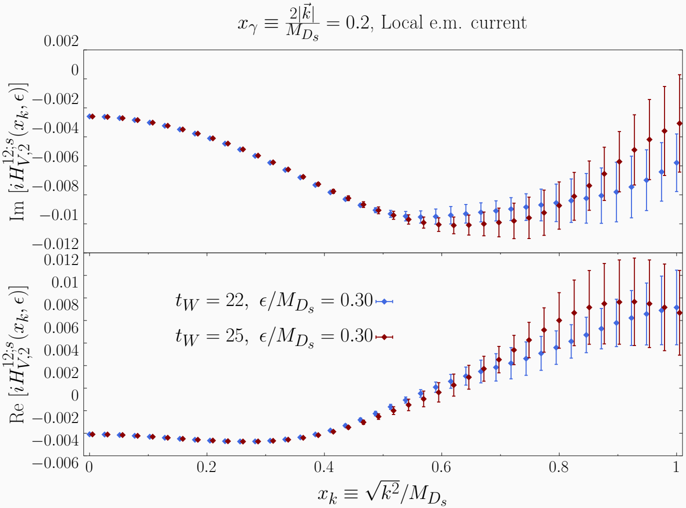

Checking ground-state isolation

H_V is given in lattice units

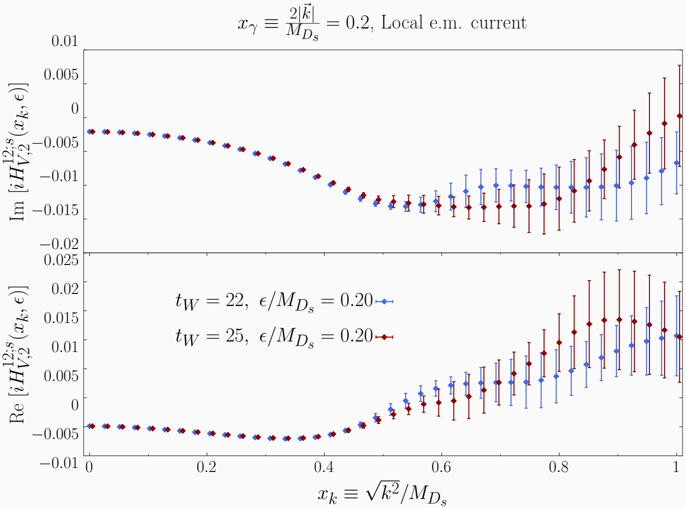

Checking ground-state isolation

H_V is given in lattice units

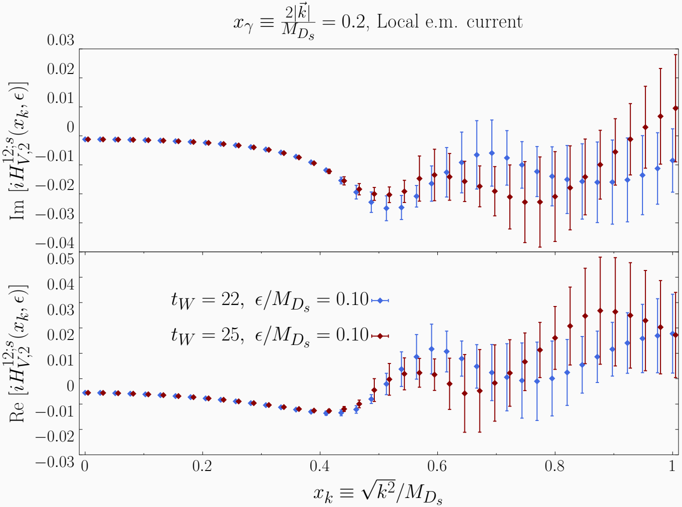

Dependence on E_{th}

H_V is given in lattice units

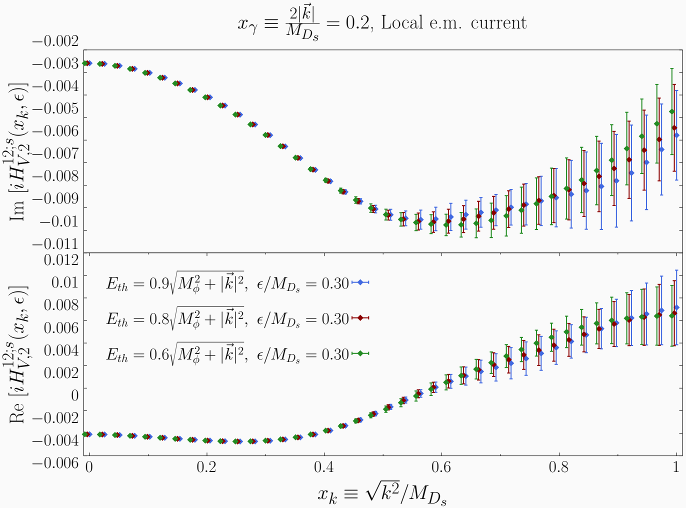

Dependence on E_{th}

H_V is given in lattice units

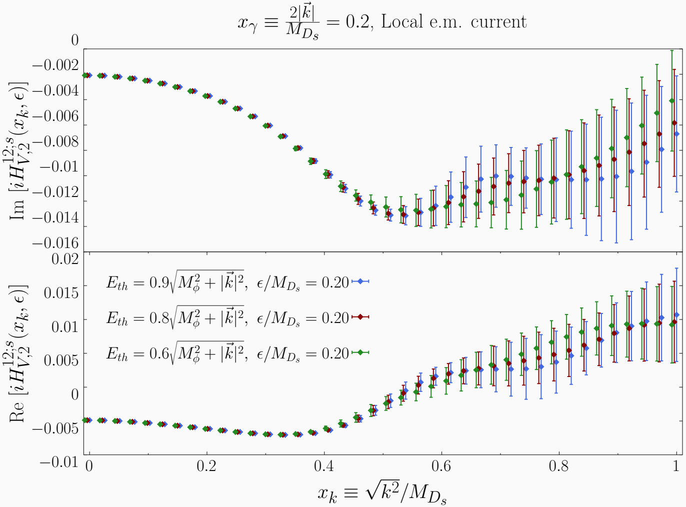

Dependence on E_{th}

H_V is given in lattice units

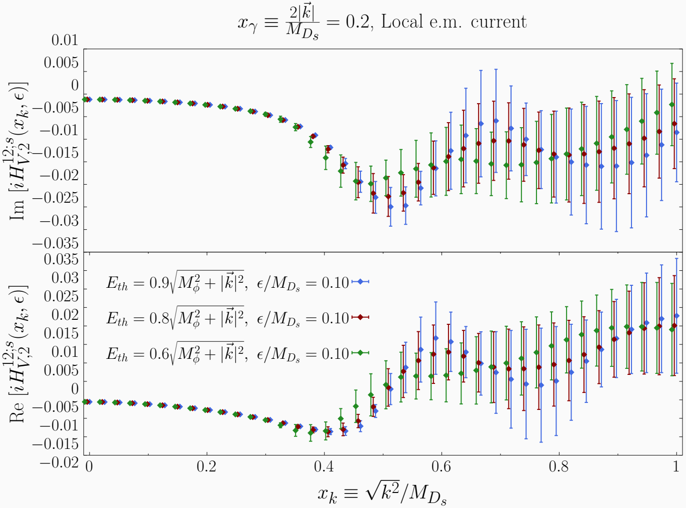

Pole model fits to F_A and F_V for real photon emission

- If single-pole model employed to describe $F_W, W = \{V, A\}$:

$$F_W(x_\gamma) = \frac{C_W}{2E^W_{pole}\left(E^W_{pole} + E_\gamma - M_{D_s}\right)}, \quad E^W_{pole} = \sqrt{(M^W_{pole})^2 + \boldsymbol{k}^2}$$

with C_W, M^W_{pole} fit parameters, we get:

$$M^A_{pole} = 2840\ (74)\ \text{MeV}, \qquad \text{expected: } M_{D_{s1}} = 2460\ \text{MeV}$$

$$M^V_{pole} = 2197\ (28)\ \text{MeV}, \qquad \text{expected: } M_{D_s^*} = 2112\ \text{MeV}$$

- Pole position closer to physical nearest resonance in vector channel. Coupling C_V related to $g_{D_s^* \to D_s\gamma}$ coupling.
- From single-pole fit, we get $g_{D_s^* \to D_s\gamma} = 0.13(1)$.
- Can be compared with direct lattice calculation ($g_{D_s^* \to D_s\gamma} = 0.11(2)$) [HPQCD Coll., 2014], and prediction from light-cone sum rule ($g_{D_s^* \to D_s\gamma} = 0.60(19)$) [Pullin and Zwicky, 2021].